Strong-field adiabatic passage in the continuum: Electromagnetically induced transparency and stimulated Raman adiabatic passage

A. Eilam[1] and M. Shapiro[1,2]

[1]*Department of Chemistry, University of British Columbia, Vancouver, British Columbia, Canada V6T1Z1*

[2]*Department of Chemical Physics, The Weizmann Institute, Rehovot 76100, Israel*

(Received 17 October 2011; published 27 January 2012)

We present a fully quantum-mechanical theory of the mutual light-matter effects when two laser pulses interact with three discrete states coupled to a (quasi)continuum. Our formulation uses a single set of equations to describe the time dependence of the discrete and continuum populations, as well as pulse propagation in electromagnetically induced transparency (EIT) and stimulated Raman adiabatic passage (STIRAP) situations, for both weak and strong laser pulses. The theory gives a mechanistic picture of the "slowing down of light" and the state of spontaneously emitted photons during this process. Surprising features regarding the time dependence of material and radiative transients as well as limitations on quantum light storage and retrieval are unraveled.

DOI: 10.1103/PhysRevA.85.012520 PACS number(s): 31.15.E−, 42.79.Pw, 29.40.−n

I. INTRODUCTION

In the past four decades a number of striking, interference-based phenomena, such as coherent population trapping (CPT) [1], electromagnetically induced transparency (EIT) [2,3], and stimulated Raman adiabatic passage (STIRAP) [4], have been extensively discussed in the literature. Although continuum states of, e.g., (spontaneously emitted) photons and/or atoms and molecules are invariably present, a comprehensive quantum-mechanical analysis of the involvement of such continuum states in adiabatic passage dynamics has only recently been presented [5]. Even that treatment was confined to the action of pulses in the *weak-field* regime. The propagation of strong laser pulses through media capable of exhibiting the above interference phenomena in the presence of a continuum has not been fully investigated.

According to the conventional view, the above phenomena are a result of interference between excitation pathways associated with a few atomic or molecular bound states [2,3,6–8], creating the so-called dark state (DS) [1,9], with the continuum's main role being that of endowing the bound states with "widths." In contrast, in the related field of laser-induced continuum structure (LICS), where a laser field creates structures in a continuum by mixing it with bound states, one treats the continuum explicitly [5,10,11].

In addition to the creation of a transparency window, EIT is also accompanied by the slowing down [12] and eventual stoppage and storage [13] of light via the STIRAP process [4]. The usual explanation of the slowing-down phenomenon is based on the the macroscopic Kramers-Kronig dispersion relations [14], which relate the steepness and slope of the dispersion curve to the light's group velocity. In this paper we strive to provide a "mechanistic" quantum-optical explanation of the effect.

A major issue associated with the slowing down of light is how to optimize the desired spectral width of the EIT transparency window relative to the spectral width of the probe pulse. Understanding this relation will help decrease the absorption losses [15–18]. It will also help decide whether it is possible to slow down and ultimately stop light in the absence of any absorption. We know that when the transparency window is wide (due to the application of a strong-"coupling" field), though the probe field experiences less absorption, there is essentially no slowing-down effect. In contrast, when the transparency window is narrow (e.g., for a weak-coupling field), though the probe field experiences more absorption, a significant slowing down of light occurs. Additional topics of interest deal with the relation between the adiabaticity of the coupling field and the efficiency of the light storage process [19,20].

In this paper we address many of these questions by developing a uniform theory of the above phenomena. We consider the situation depicted in Fig. 1 in which two ("probe" and "coupling") propagating laser pulses of arbitrary strengths act on three Λ-configuration material states. These states are coupled to a radiative (or nonradiative) (quasi)continuum. In the present case the (quasi)continuum is the (spontaneously emitted) one-photon states of the radiative modes in a cavity. By representing the continuum as a dense set of discrete levels we are able to formulate a complete description of EIT, including the dynamics of ("virtual") photons during propagation, the slowing down of light, and the eventual stopping and "storage" of light via the STIRAP process.

This paper is organized as follows: in Sec. II we explain how the continuum is incorporated into the equations describing the population and propagation dynamics. In Sec. III A we present time-dependent results for the response of the material system to the combined effect of a strong probe and a strong-coupling pulse. In Sec. III B we study propagation effects in the light storage-retrieval process. Concluding remarks are made in Sec. IV.

II. THEORY

We consider the action of two (probe and coupling) laser pulses of electric fields $\varepsilon_i(t), i = p,c$, on the system depicted in Fig. 1, composed of three bound states $|j\rangle, j = 1,2,3$ (of energies $E_1 < E_2 < E_3$), and a continuum of $|k\rangle$ states (of energies $E_k = \hbar ck$). In this scheme the probe's center frequency ω_p, defined via the relation $\varepsilon_p(t) \equiv R_e\mathcal{E}_p(t)\exp[-i(\omega_p t - k_p x + \phi_p)]$ is in near resonance with the $|1\rangle \leftrightarrow |3\rangle$ transition, i.e., $\omega_p \approx (E_3 - E_1)/\hbar$, whereas the

 ©2012 American Physical Society

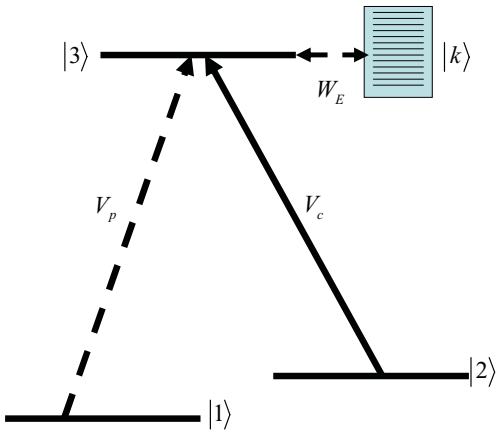

FIG. 1. (Color online) A schematic description of a three-level Λ system plus a continuum. State $|1\rangle$ ($|2\rangle$) is coupled radiatively via the V_p (V_c) term to the higher $|3\rangle$ state, which in turn is coupled via the W_E terms to the (quasi)continuum states $|k\rangle$.

coupling-laser center frequency ω_c is in near resonance with the $|2\rangle \leftrightarrow |3\rangle$ transition, $\omega_c \approx (E_3 - E_2)/\hbar$.

The Hamiltonian entering the time-dependent Schrödinger equation,

$$i\hbar\frac{\partial}{\partial t}|\Psi\rangle = H|\Psi\rangle, \tag{1}$$

is written as

$$H = H_0 + |1\rangle V_p\langle 3| + |2\rangle V_c\langle 3| + \sum_k |3\rangle W_k\langle k| + \text{H.c.}, \tag{2}$$

where H_0 is the nonradiative part and

$$V_i(t) = \mu_i\mathcal{E}_i(t)/2\hbar, i = p,c, \tag{3}$$

are two (Rabi frequencies) terms that radiatively couple level 1 to level 3 and level 2 to level 3. W_k are the terms coupling level 3 to the continuum. The system wave function Ψ is expanded as a superposition of three material discrete states and a set of $N \approx 600$ (quasi)continuum states.

$$|\Psi\rangle = \sum_{i=1}^{3} a_i|i\rangle + \sum_{k=1}^{N} b_k|k\rangle. \tag{4}$$

The quasicontinuum states represent any (ionization, spontaneous emission, dissociation) continuum to which the system is coupled. This number of the quasicontinuum states in addition to the coupling W_k and the energy spacing Δ_k represents ideally any kind of continuum and remains in a convergence test compared to a higher number of states. In the present application the continuum is mainly perceived as corresponding to the population by a single spontaneously emitted photon of all the radiative modes available to the system.

Substituting Eq. (4) in Eq. (1), we obtain in the rotating-wave approximation (RWA):

$$i\hbar\frac{d}{dt}a_1 = -\Delta_p a_1 + V_p{}^* a_3 - i\gamma_1 a_1,$$
$$i\hbar\frac{d}{dt}a_2 = -\Delta_c a_2 + V_c{}^* a_3 - i\gamma_2 a_2,$$
$$i\hbar\frac{d}{dt}a_3 = V_p a_1 + V_c a_2 + \sum_k W_k{}^* b_k,$$
$$i\hbar\frac{d}{dt}b_k = \Delta_k b_k + W_k a_3, k = 1,\ldots,N,$$

where we have added two small decay terms γ_j to simulate the collisional relaxations of the $j = 1,2$ lower states. In the above $\Delta_k = (E_k - E_3)/\hbar$, while $\Delta_p = \omega_p - (E_3 - E_1)/\hbar$ and $\Delta_c = \omega_c - (E_3 - E_2)/\hbar$ are the detunings from one photon resonance of the two fields. For simplicity we normalize all the time and frequency components by $\Gamma' = 100\gamma$, where $\gamma_1 = \gamma_2 = \gamma$. We define $t = t\Gamma'$, $E = E/\hbar\Gamma'$, and $V_j = V_j/\Gamma'$. The populations in the discrete states are given as $|a_i(t)|^2$, with the coherences between discrete states being given as $a_i{}^* a_j$. Energy conservation dictates that the asymptotic population of the continuum states, given as $|b_k(t \to \infty)|^2$, is equal to the total photoabsorption experienced by the external (probe and coupling) pulses. We therefore call $|b_k(t \to \infty)|^2$ resulting from placing the probe-pulse center frequency at the center of the EIT transparency window the "absorption spectrum."

III. RESULTS

A. Time-dependent results

In the first application of the above formulation we solve the time-dependent material equations (using a straightforward propagation code) for a probe laser whose pulse width is much larger than the transparency window and a coupling laser described by a monochromatic (cw) field. In Fig. 2 we display the total absorption spectrum, i.e., the probability of ending up at asymptotic times ($t \to \infty$) in the $|k\rangle$ continuum states. The curves appear identical to the usual weak-field EIT absorption spectrum, obtained by scanning a probe pulse of

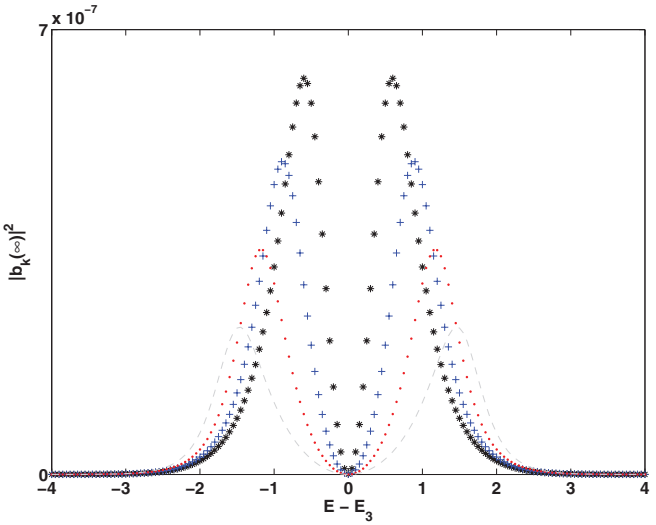

FIG. 2. (Color online) The pulse absorption, given as $|b_k(\infty)|^2$, the population of the spontaneously emitted one-photon continuum with $k = E/(\hbar c)$, for a broadband pulse (FWHM $= 2\Gamma'$) whose center frequency coincides with the center of the EIT transparency window for several coupling field strengths. Black asterisks, $V_c = 0.6\Gamma'$; blue crosses, $V_c = 0.9\Gamma'$; red dots, $V_c = 1.2\Gamma'$; gray dashed line, $V_c = 1.5\Gamma'$. $W_k = 0.05\Gamma'$, $\Delta_k = 0.01\Gamma'$, and $E - E_3$ is in units of $\hbar\Gamma'$.

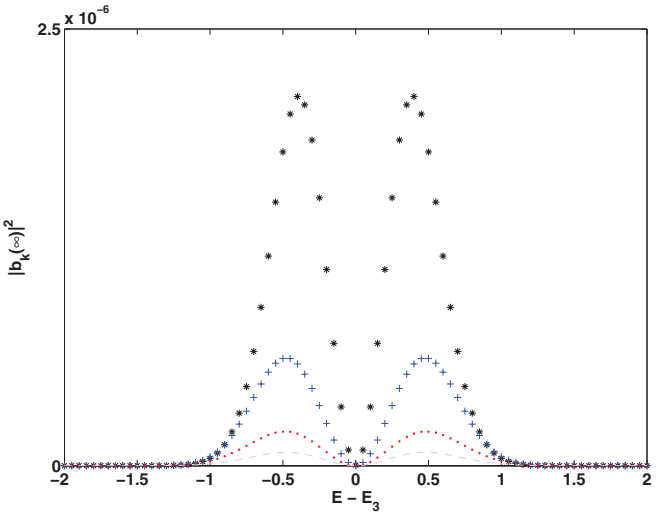

FIG. 3. (Color online) The total absorption spectrum, given as the $|b_k(\infty)|^2$ continuum coefficients, for a pulse whose spectral bandwidth is comparable to that of the EIT transparency window (FWHM $\approx 0.6\Gamma'$) for several amplitudes of the coupling field: $V_c = 0.6\Gamma'$ (black asterisks), $0.9\Gamma'$ (blue crosses), $1.2\Gamma'$ (red dots), and $1.5\Gamma'$ (gray dashed line). The energy units are defined in Fig. 2.

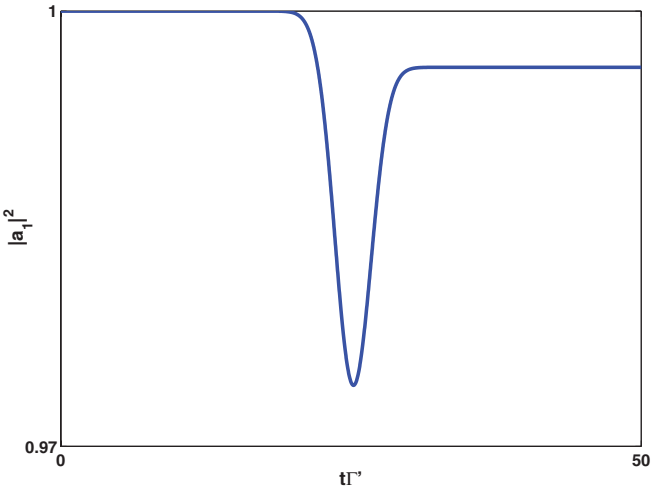

FIG. 4. (Color online) The $|1\rangle$ population as a function of normalized time for a probe pulse whose center frequency and width (FWHM $= 0.6\Gamma'$) coincide with those of the transparency window. We see a transient loss (of about 2.5%) of the $|1\rangle$ population at the peak of the pulse. This loss is almost entirely regained (except for a permanent loss of about 0.5% due to absorption at the tails of the pulse) at the end of the pulse.

infinitesimal width across E. We see a transparency window in the absorption spectrum whose width, given by the Autler-Townes (AT) splitting of the excited state, gets larger and larger as we increase the coupling-laser field strength.

When these calculations are repeated for a probe pulse whose width is comparable to the EIT transparency window, the results are not identical to the previous case, as shown in Fig. 3. Though as before the height of the two peaks is reduced as we increase the coupling-laser strength, here the separation between the two peaks remains roughly the same. This reduction in the area under the peaks means that fewer and fewer probe photons are absorbed as the coupling-laser intensity increases.

This result can be understood analytically using a recent derivation of the probe-pulse absorption spectrum [5], according to which

$$P_{abs}(E) = \frac{2\pi\Gamma|\mu_p\epsilon_p(\omega_{E,1})|^2[(E-E_3)^2]}{\left[(E-E_3)^2 - V_c^2\right]^2 + [(E-E_3)\Gamma/2]^2}. \quad (5)$$

The limited bandwidth of the probe pulse [expressed in the above formula as $\epsilon_p(\omega_{E,1})$] curbs the separation between the two AT components as the intensity of the coupling laser (i.e., V_c) is increased.

We next present a set of computations of the transient behavior of the population of state $|1\rangle$. First, we present the transient behavior of the population of state $|1\rangle$ in Fig. 4 for $V_c = 1\Gamma'$ and $V_p = 0.1\Gamma'$. Contrary to common belief, even in EIT, a strong probe pulse can cause a certain amount of transient absorption of the $|1\rangle$ state. If, however, the pulse is centered at the transparency window, the $|1\rangle$ state gets almost completely repopulated as the pulse wanes. Some population does get lost at long times due to the overlap of the tails of the probe pulse with the region outside the transparency window.

One of the main results of this paper is displayed in Figs. 5 and 6, where we plot the energetic distribution of the continuum, given by $|b_k(t)|^2$, *during* the interaction of the probe pulse with the Λ system.

Quite clearly and in contradistinction to theories that do not treat the continuum dynamically, absorption at the EIT transparency dip *occurs* during the pulse. This absorption is *transient* because, as shown in Figs. 5 and 6, at the center of the EIT dip the continuum coefficients get completely *depopulated* as the probe pulse wanes, giving rise to the familiar complete transmission.

The behavior displayed in Figs. 5 and 6 gives a full mechanistic understanding of the slowing down of light, which is also discussed in the next section. We see that,

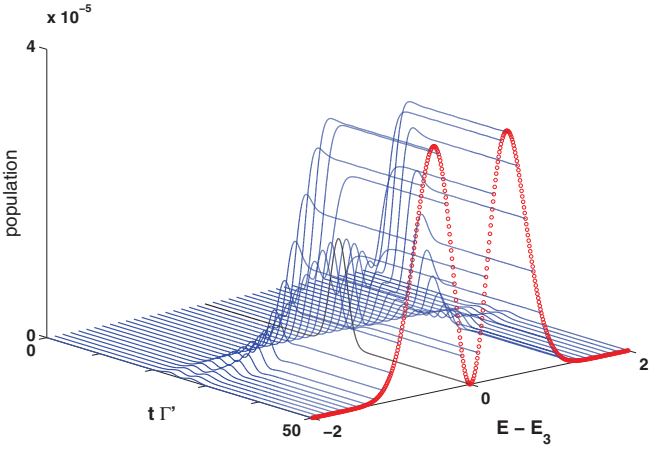

FIG. 5. (Color online) The time-dependent $|b_k(t)|^2$ continuum coefficients during the interaction of a probe pulse and a strong ($V_c = 1\Gamma'$) coupling field with the three-level system. The black line shows the on-resonance component, which, although, as expected, is unpopulated after the pulse, gets populated during the pulse. The energy units are defined in Fig. 2.

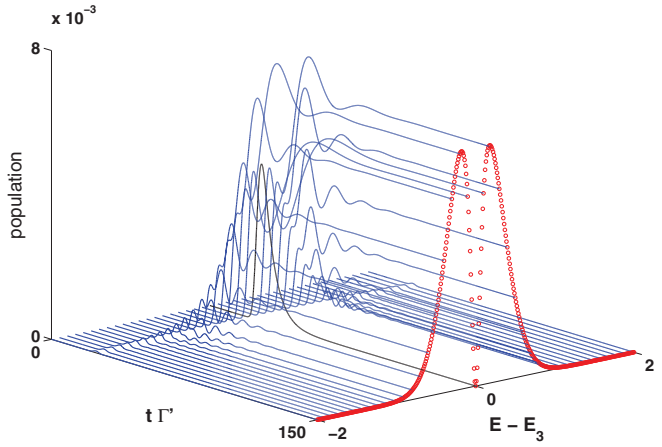

FIG. 6. (Color online) The same as in Fig. 5 for a weak ($V_C = 0.25\Gamma'$) coupling field.

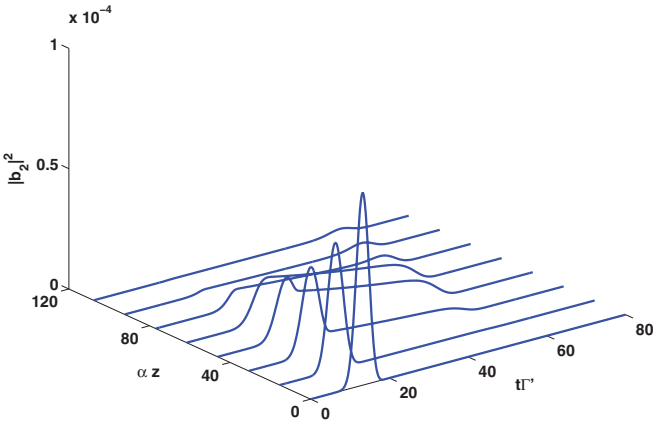

FIG. 7. (Color online) The population of state $|2\rangle$ as a function of retarded time and normalized propagation distance during the storage process, where field amplitudes are $V_c = 1\Gamma'$ and $V_p = 0.01\Gamma'$. We see the propagation of a coherent passage of population from $|1\rangle$ to $|2\rangle$ that lasts until decay due to (the assumed) decoherence rate γ_2 setting in.

as in all dispersion-type phenomena, light gets "detained" by being absorbed and (coherently) reemitted in a transient way, thereby slowing down its propagation. The slowing down is so dramatic in EIT because, contrary to ordinary dispersion, here the transient light absorption occurs *near resonance* with the material transition at $E_k = E_3 - E_1$. In contrast, in ordinary dispersion of transparent materials, the transient absorption and reemission occur at way off-resonance frequencies (relative to the material transition frequencies). As a result, the slowing-down effect is not nearly as dramatic.

Comparing Figs. 5 and 6, we see that, as the coupling laser becomes weaker, the whole structure becomes, as expected, narrower. What is entirely different, and of equal significance, is that, for the weaker-coupling pulse, the on-resonance continuum transient (the black line in Figs. 5 and 6) rises *higher* and lasts almost *three times* longer compared to the strong-coupling case. Thus a larger fraction of the probe photons suffer absorption and reemission, and the whole process lasts longer for weak pulses, detaining the probe light further and further, i.e., slowing the light more and more, as the coupling laser gets weaker and weaker. An additional interesting effect associated with the lengthening of the transients is the extra oscillations in the *off-resonance* components before they finally settle down to their familiar EIT absorption spectrum. We also notice that the spectral width of the spontaneously emitted one-photon transients is significantly larger than the final EIT line shape. This means that the probe pulse is accompanied by a transient "halo" of spontaneously emitted off-resonance photons, part of which is being reabsorbed as the pulse departs the three-level system.

B. Temporal and propagation effects during light storage and retrieval

We now examine the propagation of pulses through the medium, the slowing down of light, and the storage and retrieval of light. In order to do so, we solve the Maxwell-Bloch equations for field propagations,

$$\left(\frac{\partial}{\partial z} + \frac{1}{c}\frac{\partial}{\partial t}\right) V_{ij} = i\alpha a_i{}^* a_j,$$

where $\alpha = \pi\omega_{ij} N \mu_{ij}^2 / c\hbar\Gamma'$ is an effective coupling constant. V_{ij} are the Rabi frequencies for the $i \leftrightarrow j$ transitions, and $a_i{}^* a_j$ are the coherences between the $|i\rangle$ and $|j\rangle$ states, calculated using Eq. (5) at each z step.

We first solve the propagation equations for the simple case of a narrow-band probe pulse whose spectrum lies within the EIT transparency window. In particular, we examine the populations in the $|3\rangle$ and the $|2\rangle$ states during the light storage process.

As we switch off V_c we initiate a STIRAP process in which the light is being absorbed via adiabatic passage from $|1\rangle$ to state $|2\rangle$, and the control field is amplified while the probe field is deamplified. This process is accompanied by the slowing down of light as $V_C \to 0$. The energy of the probe field is transferred to the writing (control) field via stimulated Raman process [19,20]. Light can be retrieved and the stored information decoded by switching back on the V_c coupling.

In order to understand the dynamics of the process we present in Figs. 7 and 8 the population in state $|2\rangle$ and in state $|3\rangle$ for a slowly varying ("adiabatic") control field. In Fig. 7 we present the population in the $|2\rangle$ state as the probe and coupling pulses propagate. We see that population accumulates in the $|2\rangle$ state due to adiabatic passage from state $|1\rangle$ during the writing process. Population flows back to the $|1\rangle$ state during the reading process. There is a loss of the population due to the assumed decoherence processes, as embodied in the γ_i parameters of Eq. (5).

In addition to the smooth adiabatic passage between the $|1\rangle$ and $|2\rangle$ states, some population is seen to be trapped transiently in the $|3\rangle$ state. The time dependence of the $|3\rangle$ population exhibits a double-peak structure. This structure is a result of the transfer of a small portion of the population to the continuum and to state $|3\rangle$ as the system transits from state $|1\rangle$ to state $|2\rangle$ and back again. As the pulses propagate further the double-peak structure is seen to break up, with the earlier peak being transferred back to state $|1\rangle$ during the reading process.

The slowing down of light during the storage process is demonstrated as a function of t and z in Fig. 9, where we plot

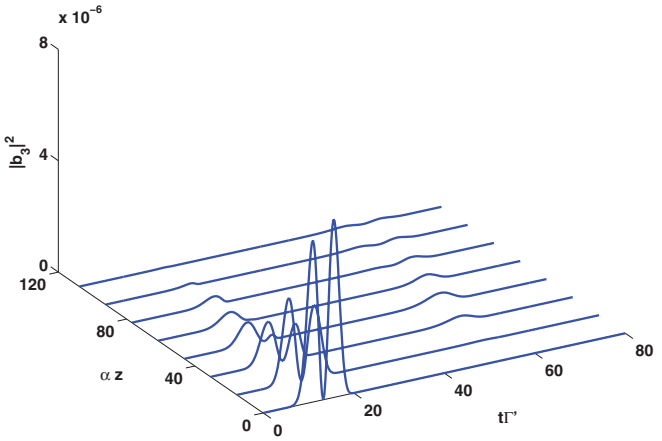

FIG. 8. (Color online) The population of the high-lying $|3\rangle$ state as a function of retarded time and normalized distance during the light storage process, where field amplitudes are $V_c = 1\Gamma'$ and $V_p = 0.01\Gamma'$. A small transient accumulation of population is seen to be transferred to this level as the system shuttles between state $|1\rangle$ and state $|2\rangle$, resulting in a double-transient-peak structure.

the position of the peak of the probe pulse during the storage process (blue dotted line) and contrast it with the behavior of a pulse (whose peak position is shown with red circles) propagating at c, the speed of light in vacuum. We clearly see that the probe pulse is stopped between $t = 20$ and $t = 60$ at which point a portion of it is regenerated to resume its slow velocity propagation.

We now turn our attention to the propagation of the continuum components. We distinguish between the three cases (see Fig. 10) according to dV_c/dt, the rate of change of the coupling-laser Rabi frequency. We term the $dV_c/dt \ll V_c\omega_c$ case *adiabatic*, the $dV_c/dt = V_c\omega_c$ case *quasiadiabatic*, and the $dV_c/dt \gg V_c\omega_c$ case *nonadiabatic*.

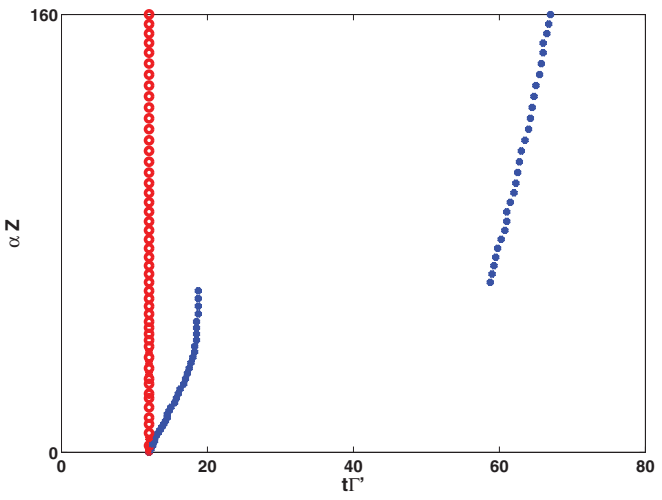

FIG. 9. (Color online) The propagation of the peak of the probe pulse during the storage process (blue dotted line) vs the peak of a pulse propagating at c, the speed of light in vacuum (line of red circles). The peak of the probe clearly experiences a great reduction in speed. At $t\Gamma' \sim 20$ (in the units of Fig. 5) the probe pulse is seen to terminate, corresponding to the stoppage of light. The probe pulse is resurrected at $t\Gamma' \sim 60$, from which point it propagates at $v \ll c$.

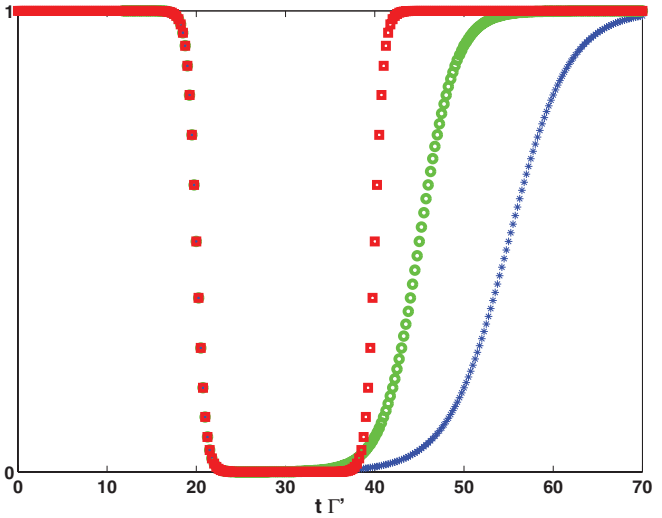

FIG. 10. (Color online) Different coupling-laser turn-on. The turn-on is parameterized as $V_c(t) = V_c\{1 - 0.5[\tanh(t - \tau_1) - \tanh k(t - \tau_2)]\}$, where $k = 1$ is the nonadiabatic case (red squares), $k = 0.5$ is the quasiadiabatic case (green circles), and $k = 0.15$ is the adiabatic case (blue asterisks).

The coupling pulse shape in the midpoints of the "encoding" (storage) and "decoding" (light retrieval) phases for the above three cases are shown in Fig 10.

The calculations show that in the adiabatic case the encoding and decoding absorption spectra are essentially identical to one another. In contrast, in the quasiadiabatic case, shown in the middle panel of Fig. 11, some differences between the encoding and the decoding absorption spectra become evident. Specifically, the decoding absorption spectrum is seen to exhibit slight undulations superimposed on the usual EIT line shape. This trend continues for the nonadiabatic

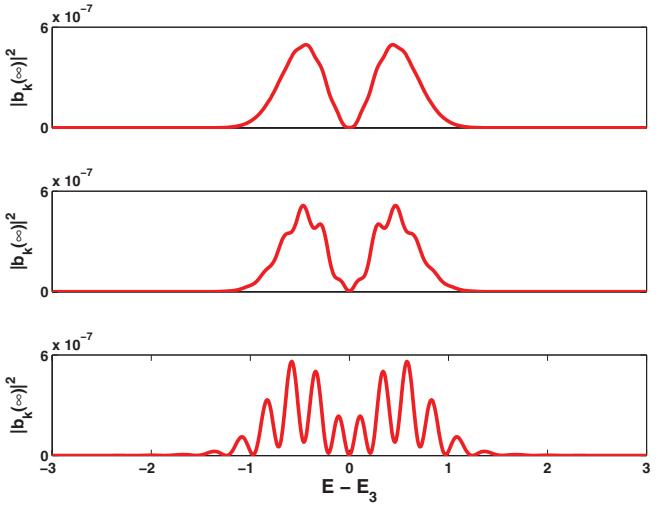

FIG. 11. (Color online) The absorption spectrum, given as the $|b_k(\infty)|^2$ continuum coefficients, in the retrieval phase. In contrast to the absorption at the storage phase, which is essentially identical to that of Fig. 3, the spectral features of the *retrieved* light are seen to depend on the coupling-laser turn-on rates. (top) The adiabatic case, (middle) the quasiadiabatic case, and (bottom) the nonadiabatic case. $E - E_3$ is in units of $\hbar\Gamma'$.

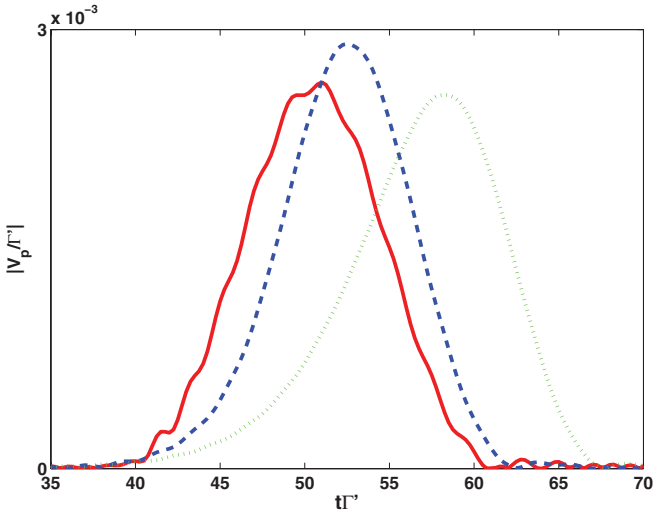

FIG. 12. (Color online) The probe field at the end of the retrieval process for three cases of the retrieval (coupling) laser. The green dotted line shows the adiabatic case, the blue dashed line shows the quasiadiabatic case, and the solid red line shows the nonadiabatic case. While the efficiency is evidently similar in all three cases, the probe field is seen to acquire additional modulations in the nonadiabatic case.

decoding process, shown in the bottom panel of Fig. 11. We see deep modulations of high visibility imprinted on a smoothly changing EIT-type envelope. No such modulations are observed for the light *encoding* absorption spectrum, which is identical to that of Fig. 3.

The difference between the encoding and decoding spectra for the nonadiabatic case is due to the fact that during the encoding process the ratio between the amplitudes of the probe and the control fields is well defined. In contrast, in the decoding process, the probe amplitude is being recreated from random fluctuations. When the switch-on is fast, the fluctuations introduce modulations that mimic the Fourier transform of $V_c(t)$.

The reason for the observed behavior in the quasiadiabatic case is that we turn on the coupling field rather slowly. This entails the presence of smaller-frequency Fourier components. Whereas our (quasi)adiabatic encoding process coincides with the results obtained in the past [21], Fig. 12 demonstrates that the nonadiabatic turn-on results in substantial distortions of the spectrum of the retrieved light, leading to a decrease of the quantum fidelity of the process.

IV. CONCLUSIONS

In this paper we have presented a *uniform* quantum theory of EIT, STIRAP, and pulse propagation of a three-level system in the presence of a continuum. Using this formulation, we have performed rigorous calculation of the absorption spectrum of the probe and coupling pulses under the familiar EIT setup, during and after the pulses. We have also performed calculations on the propagation of the pulses, with special emphasis on the light storage and retrieval periods.

By including the continuum in a dynamical way we have been able to show that many of the preconceptions, particularly the lack of absorption at frequencies corresponding to the EIT transparency window, are not strictly true. We have found that during the pulse, transient absorption, followed by reemission, occurs, though the net absorption at the end of the pulse does, indeed, go to zero. This finding gives a simple and detailed explanation to the dramatic slowing down of light that accompanies the EIT process. Our formulation includes STIRAP as a special case, and we find that, contrary to preconceptions based on continuum-free theories, during the STIRAP process the presence of the continuum causes the intermediate state to be populated and depopulated during the pulse in a transient way.

We have also shown that when there is a rapid shutdown of the coupling laser, which after some delay is followed by a rapid start-up of that laser, the spectra of the continuum components (and the retrieved probe pulse) contain rapid oscillations, superimposed on the usual EIT line shape (and on the probe-pulse envelope). Hence the potential use of ultrashort pulses in storing quantum information may be severely limited.

[1] E. Arimondo and G. Orriols, Lett. Nuovo Cimento Soc. Ital. Fis. **17**, 333 (1976).
[2] S. E. Harris, Phys. Today **50**(7), 36 (1997).
[3] M. Fleischhauer, A. Imamoglu, and J. Marangos, Rev. Mod. Phys. **77**, 633 (2005).
[4] K. Bergmann, H. Theuer, and B. Shore, Rev. Mod. Phys. **70**, 1003 (1998).
[5] M. Shapiro, Phys. Rev. A **75**, 013424 (2007).
[6] S. Autler and C. Townes, Phys. Rev. **100**, 703 (1955).
[7] M. Shuker, O. Firstenberg, Y. Sagi, A. Ben-kish, N. Davidson, and A. Ron, Phys. Rev. A **78**, 063818 (2008).
[8] A. K. Patnaik, P. S. Hsu, G. S. Agarwal, G. R. Welch, and M. O. Scully, Phys. Rev. A **75**, 023807 (2007).
[9] U. Fano, Phys. Rev. **124**, 1866 (1961).
[10] M. Shapiro, J. Chem. Phys. **56**, 2582 (1972).
[11] P. Knight, Phys. Rep. **190**, 1 (1990).
[12] L. V. Hau, S. E. Harris, Z. Dutton, and C. H. Behroozi, Nature (London) **397**, 594 (1999).
[13] M. Fleischhauer and M. D. Lukin, Phys. Rev. Lett. **84**, 5094 (2000).
[14] R. W. Boyd, D. J. Gauthier, A. L. Gaeta, and A. E. Willner, Phys. Rev. A **71**, 023801 (2005).
[15] V. Boyer, C. F. McCormick, E. Arimondo, and P. D. Lett, Phys. Rev. Lett. **99**, 143601 (2007).
[16] I. Novikova, D. F. Phillips, and R. L. Walsworth, Phys. Rev. Lett. **99**, 173604 (2007).
[17] A. Eilam, A. D. Wilson-Gordon, and H. Friedmann, Opt. Lett. **33**, 1605 (2008).
[18] R. M. Camacho, P. K. Vudyasetu, and J. C. Howell, Nat. Photonics **3**, 103 (2009).
[19] A. B. Matsko, Y. V. Rostovtsev, O. Kocharovskaya, A. S. Zibrov, and M. O. Scully, Phys. Rev. A **64**, 043809 (2001).
[20] T. N. Dey and G. S. Agarwal, Phys. Rev. A **67**, 033813 (2003).
[21] M. Fleischhauer and M. D. Lukin, Phys. Rev. A **65**, 022314 (2002).